



# Sustainable method for Alzheimer's prediction in Mild Cognitive Impairment: EEG connectivity and graph theory combined with ApoE

Fabrizio Vecchio<sup>1</sup>, Francesca Miraglia<sup>1,3</sup>, Francesco Iberite<sup>1</sup>, Giordano Lacidogna<sup>2</sup>, Valeria Guglielmi<sup>2</sup>, Camillo Marra<sup>2,3</sup>, Patrizio Pasqualetti<sup>4</sup>, Francesco Danilo Tiziano<sup>5</sup> and Paolo Maria Rossini<sup>3</sup>

*1) Brain Connectivity Laboratory, IRCCS San Raffaele Pisana, Rome, Italy*

*2) Neuropsychological Center- Catholic University – Rome*

*3) Institute of Neurology, Area of Neuroscience, Catholic University, Policlinic A. Gemelli Foundation, Rome, Italy*

*4) Service of Medical Statistics and Information Technology, Fatebenefratelli Foundation for Health Research and Education, AFaR Division, Rome, 00186 Italy.*

*5) Institute of Medical Genetics, Catholic University, Policlinic A. Gemelli Foundation, Rome, Italy*

**Running title:** Brain networks related to MCI conversion

**Key words:** precision medicine; graph theory; Alzheimer; MCI; functional connectivity; EEG; alpha band; eLORETA; conversion; ApoE

**Corresponding author:**

Prof. Paolo Maria Rossini.

Institute of Neurology, Area of Neuroscience  
Catholic University, Policlinic A. Gemelli Foundation,  
Rome, Italy

E-mail: [paolomaria.rossini@policlinicogemelli.it](mailto:paolomaria.rossini@policlinicogemelli.it)

This article has been accepted for publication and undergone full peer review but has not been through the copyediting, typesetting, pagination and proofreading process, which may lead to differences between this version and the Version of Record. Please cite this article as doi: 10.1002/ana.25289

## Abstract

Mild cognitive impairment (MCI) is a condition intermediate between physiological brain aging and dementia. Amnesic-MCI (aMCI) subjects progress to dementia (typically to Alzheimer-Dementia=AD) at an annual rate which is 20 times higher than that of cognitively intact elderly. The present study aims to investigate whether EEG network Small World properties (SW) combined with Apo-E genotyping, could reliably discriminate aMCI subjects who will convert to AD after approximately a year. 145 aMCI subjects were divided into two sub-groups and, according to the clinical follow-up, were classified as Converted to AD(C-MCI, 71) or Stable(S-MCI, 74). Results showed significant differences in SW in delta, alpha1, alpha2, beta2, gamma bands, with C-MCI in the baseline similar to AD. Receiver Operating Characteristic(ROC) curve, based on a first-order polynomial regression of SW, showed 57% sensitivity, 66% specificity and 61% accuracy(area under the curve: AUC=0.64). In 97 out of 145 MCI, Apo-E allele testing was also available. Combining this genetic risk factor with Small Word EEG, results showed: 96.7% sensitivity, 86% specificity and 91.7% accuracy(AUC=0.97). Moreover, using only the Small World values in these 97 subjects, the ROC showed an AUC of 0.63; the resulting classifier presented 50% sensitivity, 69% specificity and 59.6% accuracy. When different types of EEG analysis (power density spectrum) were tested, the accuracy levels were lower (68.86%). Concluding, this innovative EEG analysis, in combination with a genetic test (both low-cost and widely available), could evaluate on an individual basis with great precision the risk of MCI progression. This evaluation could then be used to screen large populations and quickly identify aMCI in a prodromal stage of dementia.

## Introduction

Mild cognitive impairment (MCI) is a clinical and neuropsychological state in the elderly brain which is intermediate between normal cognition and dementia. It is mainly characterized by objective evidence of memory impairment during a neuropsychological examination that does not yet encompass the definition of dementia<sup>1,2</sup>. Epidemiological research suggests that amnesic MCI (aMCI) is a precursor to Alzheimer's Dementia (AD)<sup>3</sup>, based on the high rate of progression from this state to AD<sup>2</sup>. About 50% of all MCI subjects convert to dementia<sup>4-7</sup>. The others will either remain in the MCI condition or return to a fully normal one and never progress to dementia.

To plan optimal and early therapeutic, organizational, lifestyle and rehabilitative interventions, aMCI diagnosis should be combined with the most reliable prognosis on the likelihood and time of progression to dementia. Growing evidence suggests that early diagnosis reduces the health and social costs associated with dementia management<sup>8,9</sup>. Moreover, prodromal MCI to AD is becoming the preferred target for clinical trials with potentially disease-modifying experimental drugs. Because such a high risk is associated with the MCI condition, it is important to increase the success rate of the trials conducted. The early diagnosis of *prodromal* MCI to AD can presently be reached with a high degree of sensitivity and specificity by combining a number of tests (e.g. hippocampal volumetric MRI, PET or PET integrated with beta-amyloid and tau radioligands and lumbar puncture for CSF beta- and tau-metabolites). Due to their high costs, limited availability and/or body invasiveness, however, these tests cannot be used to screen a large population sample.

Electroencephalogram (EEG) is an ideal candidate for such screening, because it is a widely available, non-invasive and low-cost<sup>10</sup> procedure. Moreover, a great deal of research has been conducted on EEG abnormalities in pathological brain aging<sup>11</sup>. AD patients show more delta and fewer posterior alpha EEG rhythms than cognitively intact elderly (Nold) subjects<sup>12</sup>.

Similarly, MCI show less alpha power than Nold subjects<sup>13</sup>. Furthermore, a reduction in EEG spectral coherence in the alpha band in AD has been reported<sup>14,15</sup>, and EEG theta power was found to be higher in aMCI subjects who will convert to AD. High predictive accuracy between baseline EEG features and the probability of a future decline was found<sup>16</sup>. Furthermore, EEG coherence has been shown to contribute to the classification of AD from Nold<sup>15</sup> and to the prediction of aMCI conversion to AD<sup>14</sup>. However, findings were usually significant only at a group level<sup>17</sup>; moreover, relatively small samples were investigated with a briefer-than-required follow up. Despite such limitations, the progression of the diagnosis of AD has been summarized in a review<sup>18</sup>, showing generalized slowing of the rhythms contained in the spectral profile, reduced complexity and perturbations in EEG organization. Furthermore, the cortico-cortical connectivity and network properties of EEG have been addressed in several studies<sup>11,19-21</sup>. Many of the studies have also explored the idea that dementias—particularly in the very early, namely prodromal, stages—mainly affect synaptic transmission and therefore represent “disconnection syndromes”<sup>22</sup>.

Network science tends to model the brain as an intricate amalgamation of networks; a network is a mathematical representation of a real-world complex system, which is defined by a collection of nodes (vertices) and links (edges) between pairs of nodes. Nodes usually represent brain regions, while links represent anatomical, functional or effective connections, depending on the dataset<sup>23</sup>. Anatomical connections typically correspond to white matter fiber tracts between pairs of grey matter brain regions (cortical areas or subcortical relays). Connections between neuronal assemblies reflect segregation and integration processes, as revealed by local clustering (segregation) and path length (integration). Brain connections are organized in a network topology characterized by a high degree of local clustering (segregation) and long-distance connections (integration). A “Small-world” concept was introduced as a model of network organization, allowing for an optimal balance between local specialization and global integration<sup>24</sup>. This approach could be used to model brain-functional architecture<sup>25</sup> and correlate

it with behavior (i.e. neuropsychological test performance). This evaluates whether functional connectivity patterns between brain areas reproduce the organization of more-or-less strictly bound networks based on the strength of oscillatory firing synchronizations between adjacent/remote neuronal assemblies in a time frame of milliseconds<sup>26-30</sup>. In recent literature several studies have utilized graph theory analysis of connectivity from EEG signals combined with ApoE genotyping in order to discriminate between healthy elderly and AD patients<sup>31,32</sup>. No previous studies utilized such an approach to distinguish *prodromal-to-AD* from *non-prodromal* –MCI subjects.

The primary aim of the present study was to investigate brain connectivity using a Small World approach for the analysis of EEG-related neural networks. Moreover, as the  $\epsilon 4$  allele of the *Apo-E* gene is a genetically determined risk factor for the pathogenesis of late-onset and sporadic AD, a secondary endpoint is to investigate whether EEG connectivity markers along with genetically determined risk-indicators for dementia, as represented by Apo-E testing can reach a greater sensitivity/specificity for the stage of MCI prodromal to AD<sup>33,34</sup>. Our purpose is to provide a reliable low-cost, widely available and non-invasive method for discrimination of high-risk aMCI subjects, namely those who, on an individual basis, will rapidly (i.e. after 1 or 2 years) convert to AD.

## Subjects and methods

### *Participants*

The ages of the 145 aMCI subjects at the time of the EEG recordings were:  $71.83 \pm 0.56$  SEM, MMSE was  $25.87 \pm 0.18$ , and gender distribution was 82 females and 63 males. The participants, all of whom were affected by aMCI, had been referred to the Memory Clinic of the Catholic University, Policlinic A. Gemelli Foundation in Rome<sup>4,35,36</sup>. They were divided into two sub-groups according to their clinical evolution, classified as converted to AD or stable aMCI after a follow-up from Time 0 (=diagnosis of MCI). At the end of the follow-up, it was shown

that at the time of the EEG recordings, the patient group included 74 stable aMCI (= aMCI-S: age  $70.72 \pm 0.77$  SEM, MMSE  $26.33 \pm 0.27$ , months of follow-up  $38.17 \pm 3.48$ ; M/F: 33/41) and 71 Converted aMCI (= aMCI-C: age  $73.05 \pm 0.81$  SEM, MMSE  $25.32 \pm 0.23$ , months of follow-up  $18.29 \pm 1.60$ ; M/F: 35/36). The time interval between aMCI diagnosis and EEG recording was less than one month in both groups and at an individual level. As an EEG control group, 175 AD age-matched patients were selected (age  $72.23 \pm 0.55$ , MMSE  $20.12 \pm 0.31$ , M/F: 81/94).

All subjects were right-handed, according to the Handedness Questionnaire. Individual informed consent was obtained, and the study was approved by a local ethical committee. Experimental procedures conformed to the Declaration of Helsinki and national guidelines.

#### *Inclusion and exclusion criteria*

All subjects took part in a battery of neuropsychological tests assessing attention, memory, executive functions, visuo-construction abilities and language. Memory was assessed via the immediate and delayed recall of the Rey Auditory Verbal Learning Test, the delayed recall of Rey figures, the delayed recall of a 3-word list and the delayed recall of a story. An MCI amnesic diagnosis hinged upon an impairment in at least one episodic memory test. The abnormal threshold for performances on the memory tasks was set below the 5th percentile of the healthy population. The exclusion criteria included traumatic head injuries, epilepsy, alcoholism and the occurrence of any other past neurological or psychiatric diseases. The patients were carefully screened for medical conditions that could potentially be associated with cognitive disturbances (i.e., renal or hepatic failure, thyroid dysfunction, and folate and/or vitamin B12 deficits).

Each subject also underwent brain MRI and SPECT, MMSE (Mini-Mental State Evaluation), a clinical dementia rating (CDR) and an assessment of their Geriatric Depression Scale (GDS), Hachinski Ischemic Score (HIS) and Instrumental Activities of Daily Living scale (IADL) to confirm the diagnosis and to exclude other causes of dementia, such as frontotemporal

dementia, vascular dementia, extrapyramidal syndromes, reversible dementias and Lewy body dementia. This was performed in order to ensure the creation of clinically homogeneous groups.

AD was diagnosed according to the National Institute on Aging-Alzheimer's Association workgroups<sup>36</sup> and the DSM IV TR criteria. Moreover, the affected individuals showed a significant reduction in hippocampal volume and an increase in the width of the temporal horn and choroidal fissure (ranging between 2 and 4 on the Likert scale). The pattern of blood flow and oxygen consumption on SPECT was abnormal as well.

The exclusion criteria for AD focused upon any evidence of (i) frontotemporal dementia, (ii) behavioral variants of frontotemporal dementia, (iii) vascular dementia, (iv) extra-pyramidal syndromes, (v) reversible dementias (including pseudodementia of depression) and (vi) Lewy body dementia.

Amnesic MCI was diagnosed according to guidelines and clinical standards<sup>2,37,38</sup>. The exclusion criteria for aMCI were: (i) mild AD, as diagnosed by standard protocols, including the National Institute on Aging-Alzheimer's Association workgroups<sup>36</sup>; (ii) clinico-instrumental evidence of concomitant dementia, such as frontotemporal, vascular and reversible dementias (including pseudo-depressive dementia), marked fluctuations in cognitive performance compatible with Lewy body dementia and/or features of mixed dementias; (iii) evidence of concomitant extra-pyramidal symptoms; (iv) clinical and indirect evidence of depression, as revealed by the GDS [scores lower than 14 (no depression)]; (v) other psychiatric diseases, including epilepsy, drug addiction, alcohol dependence or the use of neuro/psychoactive drugs (including acetylcholinesterase inhibitors); and (vi) current or previously uncontrolled or complicated systemic diseases (including diabetes mellitus) or traumatic brain injuries.

Follow-up visits, including neuropsychological tests, were carried out every six months in order to intercept the epoch of an eventual MCI-to-AD conversion.

#### *Data recordings and preprocessing*

The EEG recording was performed at rest, on individuals with closed eyes and no-task conditions (for at least 5 minutes). The subjects were seated and relaxed in a sound-attenuated and dimly lit room. Electroencephalographic signals were recorded with a standard montage from 19 electrodes (Fp1, Fp2, F7, F8, F3, F4, T3, T4, C3, C4, T5, T6, P3, P4, O1, O2, Fz, Cz and Pz) positioned on the scalp, according to the International 10-20 system. Eye movements were monitored from two different channels with vertical and horizontal montages. Skin/electrode impedances were lowered below 5 K $\Omega$ .

Data were analyzed with Matlab R2011b software (Math Works, Natick, MA) using scripts from the EEGLAB 11.0.5.4b toolbox (Swartz Center for Computational Neurosciences, La Jolla, CA; [scn.ucsd.edu/eeglab](http://scn.ucsd.edu/eeglab)). The EEG recordings were band-pass filtered from 0.2 to 47 Hz using a finite impulse response (FIR) filter and a 256 Hz sampling rate. Ocular, muscular, cardiac and other types of artifacts were inspected on imported data fragmented in 2 s duration epochs. The procedure was as follows: 1) the data were reviewed, and the epochs with aberrant waveforms or with evident artifactual activity were manually discarded by an expert in EEG; and 2) the detection and rejection of artifacts were completed through an independent component analysis (ICA) using the Infomax ICA algorithm, as implemented in the EEGLAB. ICA is a blind source decomposition algorithm that enables the separation of statistically independent sources from multichannel data. It is considered an effective method for separating ocular movements and blink artifacts from EEG data. The components were visually inspected, and, if artifact contamination was found, they were manually rejected by the investigator.

#### *Functional connectivity analysis*

EEG functional connectivity analysis was performed using eLORETA exact low resolution electromagnetic tomography software<sup>26,27,39,40</sup>. The eLORETA algorithm is a linear inverse solution for EEG signals with no localization error that can indicate sources under ideal (noise-free) conditions<sup>41</sup>. According to the scalp-recorded EEG potential distribution, the low resolution

brain electromagnetic tomography (eLORETA) software was used to compute a discrete, three-dimensionally (3D) distributed linear, weighted, minimum-norm inverse solution. The particular weights used in eLORETA endow the tomography with the property of exact localization necessary to test point sources, yielding images of the current density with exact localization, albeit with a low spatial resolution (i.e. the neighboring neuronal sources are highly correlated).

To obtain a topographic view of the whole brain, brain connectivity was computed with eLORETA software in 84 regions, positioning the center in the available 42 Brodmann Areas (BAs: 1, 2, 3, 4, 5, 6, 7, 8, 9, 10, 11, 13, 17, 18, 19, 20, 21, 22, 23, 24, 25, 27, 28, 29, 30, 31, 32, 33, 34, 35, 36, 37, 38, 39, 40, 41, 42, 43, 44, 45, 46, 47) in the left and right hemispheres.

Regions of Interest (ROIs) are needed for estimation of the electric neuronal activity that is used to analyze brain-functional connectivity. The signal at each cortical ROI consisted of the average electric neuronal activities of all voxels belonging to that ROI, as computed with eLORETA. For each hemisphere, among the eLORETA current density time series of the 84 ROIs, the intracortical Lagged Linear Coherence, extracted via the “all nearest voxels” method<sup>42</sup>, was computed between all possible pairs of the 84 ROIs for each of the seven independent EEG frequency bands of delta (2–4 Hz), theta (4–8 Hz), alpha 1 (8–10.5 Hz), alpha 2 (10.5–13 Hz), beta 1 (13–20 Hz), beta 2 (20–30 Hz) and gamma (30–45 Hz) for each subject.

Starting with the definition of the complex valued coherence between time series  $x$  and  $y$  in the frequency band  $\omega$ —which is based on the cross-spectrum given by the covariance and variance of the signals—the lagged linear coherence in the frequency band  $\omega$  is reported in accordance with the following equation<sup>42</sup>:

$$LagR_{xyw}^2 = \frac{[ImCov(x,y)]^2}{Var(x)+Var(y)-[ReCov(x,y)]^2}$$

Where Var and Cov are the variance and covariance of the signals.

This was developed as a measure of true physiological connectivity not affected by volume conduction and low spatial resolution<sup>42</sup>. The values of lagged linear connectivity computing

between all pairs of ROIs for each frequency band were used as weights of the networks built in the graph analysis.

### *Graph analysis*

As previously stated, a network is a mathematical representation of a real-world complex system. It is defined by a collection of nodes (vertices) and links (edges) between pairs of nodes. Nodes usually represent brain regions, while links represent anatomical, functional or effective connections<sup>23</sup>, depending on the dataset. Anatomical connections typically correspond to white matter fiber tracts between pairs of grey matter brain regions (cortical areas or subcortical relays). Functional connections correspond to magnitudes of temporal correlations in activity and may occur between pairs of anatomically unconnected regions.

A weighted graph is a mathematical representation of a set of elements (vertices) that may be linked through connections of variable weights (edges).

In the present study, the weighted and undirected networks were built (the vertices of the network were the estimated cortical sources in the BAs) and the edges were weighted by the Lagged Linear value within each pair of vertices. The software instrument used here for the graph analysis was the Brain Connectivity Toolbox (BCT, [brain-connectivity-toolbox.net](http://brain-connectivity-toolbox.net)), adapted with our own Matlab scripts.

The Small World (SW) parameter was evaluated on the brain networks, since it measures the balance between local connectedness and the global integration of a network, representing brain network organization. Small-world architecture is intermediate between that of random networks (associated with a short overall path length but a low level of local clustering) and regular networks or lattices (which have a high level of clustering but a high overall path length); specifically, small world networks have a relatively high level of clustering and a short path length<sup>43</sup>. The measure of network small-worldness was defined as the ratio of the normalized Clustering Coefficient  $C_w$  and the normalized Path Length  $L_w$ . We used data normalization (i.e.

relativization) before performing the small-world measurements. The normalized Characteristic path length was obtained dividing the parameter by a mean value. The mean value is the average of the Characteristic path length values of each subject within the seven EEG frequency bands. The same procedure was applied to compute the normalized Clustering coefficient. As we computed from weighted networks it was difficult to evaluate disgraphs with the same number of nodes and connections (all connections were available), so we decided to use relative values within bands<sup>11,19-21</sup>.

#### *Apo-E testing*

In a subgroup of 97 subjects (age  $71.46 \pm 0.66$  SEM, MMSE  $25.98 \pm 0.22$ ; 52 stable aMCI (age  $69.85 \pm 0.89$ , MMSE  $26.74 \pm 0.29$ , months of follow-up  $45.87 \pm 3.94$ ; M/F: 22/30) and 45 Converted aMCI (age  $73.33 \pm 0.92$ , MMSE  $25.11 \pm 0.27$ , months of follow-up  $19.75 \pm 1.82$ ; M/F: 19/26), blood genotyping was performed. The Apo-E genotype was determined following the well-established method pioneered by Hixson and Vernier<sup>44</sup>. During a further classification process, we considered the MCI subjects to be “Apo-E4 non-carriers” (absence of the  $\epsilon 4$  allele) or “Apo-E4 carriers” (presence of at least one  $\epsilon 4$  allele).

#### *Statistical evaluation*

The eLORETA statistical evaluation was performed using a graph analysis pattern extracted with sLORETA/eLORETA from the brain network. The normality of the data was tested using the Kolmogorov-Smirnov test, and the hypothesis of Gaussianity could not be rejected. In order to confirm the working hypothesis, a statistical ANOVA design was addressed for the Small World between the factors Group (MCI-C, MCI-S) and Band (delta, theta, alpha 1, alpha 2, beta 1, beta 2, and gamma). An ANOVA design was also incorporated for the Small World between the factors Group (AD, MCI-C, MCI-S) and Band (delta, theta, alpha 1, alpha 2, beta 1, beta 2, gamma).

## *Polynomial Regression and ROC curve and 10-fold cross validation*

The dataset contains the small-world value of the brain network for the 145 subjects at the 7 given EEG frequency bands: delta, theta, alpha 1, alpha 2, beta 1, beta 2 and gamma. Each subject has been assigned a label according to whether he or she developed Alzheimer's disease at the follow-up.

A simple polynomial regression has been chosen, calculated using the MATLAB built-in function “fitlm”—the function fits, using the least squares method, a given polynomial. The polynomial contains 8 coefficients: the constant term and a coefficient for each of the frequency bands. The residuals plot showed an almost normal distribution, suggesting that an appropriate polynomial was chosen for the approximation.

The data were randomly distributed across the 10 groups in accordance with the “10-fold cross-validation” technique, and the classifier was tested against all of the groups while being trained on the other 9. The resulting performances and AUCs were averaged to compute the final value.

The following indexes measured the performance of the conversion binary classification:

1) Sensitivity, which measures the rate of the positives (Converted MCI) who were correctly classified as positives (i.e. they were assigned a “true positive rate” using the signal detection theory); 2) Specificity, which measures the rate of the negatives (Stable MCI) who were correctly classified as negatives (i.e. they were assigned a “true negative rate” using the signal detection theory); 3) Accuracy of the classifier (subjects correctly classified); and 4) Area under the ROC curve (AUC). We reported sensitivity, specificity and accuracy only for the “optimal” values (with the cut-off point corresponding to the maximal accuracy).

Finally, we included Apo-E genotyping in the dataset. The dataset contained the same small-world value of the brain network for the 97 subjects at the 7 given EEG frequency bands: delta, theta, alpha 1, alpha 2, beta 1, beta 2 and gamma. Added to the code of “*APO-E-ε4 non-*

*carrier*” or “*APO-E-ε4 carrier* was a polynomial containing 9 coefficients: the constant term, the Apo-E and a coefficient for each of the frequency bands. Each subject was assigned a label corresponding to the outcome (i.e. whether the individual had converted to Alzheimer’s disease at the follow-up).

## **Results**

### *Clinical data*

The clinical and demographic data of the whole group of subjects are reported in table 1, showing that the two groups present no differences.

**Insert table 1 about here**

### *Graph theory parameter analysis*

Both the ANOVAs for the evaluation of the Clustering Coefficients ( $C_w$ ) and Path Lengths ( $L_w$ ) showed statistically significant interactions ( $C_w$ :  $F(6,858)=3.7042$ ;  $p=0.00122$ ;  $L_w$ :  $F(6,858)=4.1535$ ;  $p<0.0004$ ) between Group (aMCI-Converted, aMCI-Stable) and EEG Band (delta, theta, alpha 1, alpha 2, beta 1, beta 2, gamma) factors. Duncan-planned post hoc testing showed higher values in both coefficients in the delta ( $p<0.04$ ) band, and lower values in alpha 1 ( $p<0.004$ ) and alpha 2 bands ( $p<0.011$ ) in MCI-C, with respect to the MCI-S subjects.

The ANOVA for the evaluation of the Small World (SW) showed a statistically significant interaction ( $F[6,858]=7.6633$ ;  $p<0.00001$ ) between the Group (aMCI-Converted, aMCI-Stable) and EEG Band (delta, theta, alpha 1, alpha 2, beta 1, beta 2, gamma) factors. Duncan-planned post hoc testing showed lower values of SW coefficients in the delta ( $p<0.034$ ), beta 2 ( $p<0.032$ ) and gamma ( $p<0.0001$ ) bands and vice versa for the higher SW in the alpha 1 ( $p<0.011$ ) and the alpha 2 frequency bands ( $p<0.0005$ ) in MCI-C, with respect to the MCI-S subjects.

In order to evaluate eventual differences in the AD condition, this second analysis was performed. For the evaluation of SW between the factors Group (AD, aMCI-C, aMCI-S) and Band (delta, theta, alpha 1, alpha 2, beta 1, beta 2, gamma), ANOVA showed a statistical interaction ( $F(12,1914)=7.5748$ ;  $p<0.00001$ ), as plotted in Figure 1. Duncan-planned post hoc testing showed no statistical differences between AD and aMCI-C subjects, except in the gamma band ( $p<0.00002$ ).

**Insert figure 1 about here**

Figure 2 reports the functional coupling distribution, as revealed by the lagged linear coherence, in all EEG frequency bands in the two subgroups of aMCI subjects. It is evident, as has already been illustrated in several previous studies (including one of ours), that Converted aMCI presents greater coupling in delta and lower in alpha than Stable aMCI.

**Insert figure 2 about here**

#### *Apo-E testing*

Among the 97 subjects with the Apo-E classification, of the 66 “Apo-E4 non-carriers” (lacking the  $\epsilon 4$  allele), 29 converted (43.9%). Meanwhile, among the 31 “Apo-E4 carriers” (with at least one  $\epsilon 4$  allele), 16 (51.6%) converted. The receiver operating characteristic (ROC, red line in Figure 3) curve showed an Area under the curve (AUC) of 0.51.

**Insert figure 3 about here**

#### *Classification between Stable and Converted individuals based on Small World*

In the classification process considering only the Small World values (145 subjects), the receiver operating characteristic (ROC, green line in Figure 3) curve showed an AUC of 0.64 (indicating moderate classification accuracy). The resulting classifier showed 57% sensitivity, 66% specificity and 61% accuracy for the classification of the aMCI state as a prodromal indicator of AD. This result was obtained when all subjects were included.

When adding Apo-E genotyping to the classification process (using 97 subjects), the ROC curve (blue line in Figure 3) showed an AUC of 0.97; the resulting classifier presented 96.7% sensitivity, 86% specificity and 91.7% accuracy, indicating very high accuracy for the classification of the aMCI state as prodromal to AD. Using only the Small World values in these 97 subjects, the ROC curve showed an AUC of 0.63; the resulting classifier presented 50% sensitivity, 69% specificity and 59.6% accuracy.

Of note, it is possible to consider the point density in the ROC curve as a measure of stability to threshold changes: in that regard, it is clear that the most stable (although not the highest performing) classifier is the one that relies only on Apo-E, as it evaluates only one variable with 1 and 0 as possible values. Comparing SW to SW + Apo-E, it is possible to state that, by adding genotype information, classification performance increases and stability improves.

#### *Control analyses*

Figure 4 illustrates the connection matrices related to the two groups of aMCI-Converted and aMCI-Stable (indicating the baseline functional network topology).

**Insert figure 4 about here**

In order to understand whether the difference in the baseline could influence the results, we selected two subgroups that were perfectly homogeneous in terms of their demographic and cognitive parameters. The subgroups included 42 aMCI-S and 43 aMCI-C. Furthermore, 27 aMCI-S and 30 aMCI-C also presented Apo-E testing values—demographic data are reported in Table 2. For the groups, we performed the same classifier procedures of the main analyses of the present study. Our results were in line with the main results, but were not as statistically significant, probably because of the small number of patients, who showed an AUC of 0.62. The

resulting classifier showed 52% sensitivity, 90% specificity and 61% accuracy. When adding Apo-E genotyping to the classification process, the ROC curve showed an AUC of 0.7; the resulting classifier presented 67% sensitivity, 93% specificity and 65% accuracy.

**Insert table 2 about here**

Is the need for a "graph theoretical" model supported by the present results? In order to answer this question, we compared the same type of classifier to other methods of EEG analysis currently used for AD studies and applied what was found to the same EEG epochs utilized for graph valuation, namely spectral coherence and power spectrum in combination with Apo-E. Our most significant result was obtained when analyzing the power density spectrum on all available subjects. We used sLORETA software to solve the EEG inverse problem within a three-shell spherical head model and to find the values of the voxel current density, to explain the EEG spectral power density recorded by the scalp electrodes. The current density at each voxel was then normalized to the power density averaged across all the frequencies (0.5–45 Hz) and across all 6,239 voxels of brain volume. After this normalization, the current density values lost their original physical dimension and were represented by an arbitrary unit scale. This procedure also reduced inter-subject variability.

In line with the low spatial resolution of the adopted technique, we used ROI marker sLORETA software to collapse the voxels of sLORETA solutions at 12 regions of interest [ROIs, 6 for the left and 6 for the right hemispheres, Brodmann areas included in the cortical regions of interest: frontal (8, 9, 10, 11, 44, 45, 46, 47), central (1, 2, 3, 4, 6), parietal (5, 7, 30, 39, 40, 43), occipital (17, 18, 19), temporal (20, 21, 22, 37, 38, 41, 42) and limbic (31, 32, 33, 34, 35, 36)] coded according to the Talairach space. The signal at each cortical ROI consists of the averaged electric neuronal activities of all voxels belonging to that ROI, as computed with sLORETA. The current densities at different voxels were then grouped to describe the cerebral activity in the following EEG frequency bands: delta (2–4 Hz), theta (4–8 Hz), low alpha (8–

10.5 Hz), high alpha (10.5–13 Hz), low beta (13–20 Hz), high beta (20–30 Hz) and gamma (30–45 Hz). The sLORETA method is a properly standardized, discrete, linear, minimum-norm, inverse-solution method that computes the three-dimensional cortical distribution of the electric neuronal source activity from the EEG recordings on the head surface<sup>45</sup>. A detailed description of the method can be found in several previous publications<sup>41</sup>.

In accordance with the data, we performed the classifier procedures of the main analyses of the present study and obtained 51.79% sensitivity, 100% specificity and 68.86% accuracy; these results are promising but show less significance than those in our proposal.

## Discussion

Alzheimer's disease (AD) is characterized by a progressive loss of memory and a deterioration of other cognitive functions. The illness has a prolonged and progressive course, and patients—if they survive long enough to experience the late form of the disease—die in a nearly vegetative state. The disease characteristics place an enormous emotional and financial burden on patients, their families and society<sup>46</sup>. In 2010, AD cost the United States an estimated \$604 billion. This number is staggering, especially in light of predictions that the number of AD cases worldwide, currently estimated at 36 million, will triple by 2050<sup>9</sup>. The U.S. costs of dementia were estimated to total \$818 billion in 2015, an increase of 35% since 2010; 86% of the expenses are incurred in high-income countries. The costs of informal care and the direct costs of social care represent similar proportions of the total cost, whereas the costs incurred by the medical sector are much lower. A threshold of US \$1 trillion will be crossed by 2018<sup>47</sup>.

The AD clinical phenotype follows a prodromal stage known as MCI, which is usually characterized by memory loss (aMCI). The identification of early biomarkers of conversion from aMCI to AD are of interest to researchers and health policy makers when the goal of early interventions is pursued. In fact, even in the absence (at the present) of a disease-modifying

therapy, it is evident that the early initiation of pharmacological and non-pharmacological treatments (including changes in lifestyle) helps to maintain personal autonomy in daily activities and significantly reduces the total costs of disease management<sup>48-50</sup>. Moreover, many of the clinical trials with potentially disease-modifying drugs target MCI subjects who are prodromal to AD, since failure has been demonstrated when the full symptomatology of AD has been already developed. Therefore, biomarkers that can carefully predict the evolution of the disease at an early stage could be instrumental in enabling early diagnosis and intervention and could be used to identify individuals who could benefit from trials with experimental drugs. This can be partly accomplished with the presently available diagnostic armamentarium (volumetric MRI, PET, PET+radioligands/Lumbar puncture for amyloid and tau metabolites), though it has a relatively low sensitivity to synaptic dysfunction (which is associated with a very early stage of pre-symptomatic AD) and is definitely expensive, limited in terms of its availability on a territorial level and relatively invasive. Because of these limitations, such a diagnostic combination is not feasible for a large population screening. A recent survey and meta-analysis yielded a prevalence of the MCI condition of 5.9% in the >60 year-old population, with a steady progression in the different age groups (4.5% 60-69, 5.8% 70-79, 7.1% 80-89; Cohort Studies Memory in an International Consortium-COSMIC)<sup>51</sup>. These represent significant numbers for a population-based screening. In recent years, progressively more attention has been paid to the electrophysiological substrate of the disease, which could be used to evaluate whether the analysis of brain electroencephalographic signals could track early progression from MCI to mild AD via large population screening. There is a growing interest in this technique because of its low cost, widespread availability and non-invasiveness. This paper aimed to determine whether a specific analysis of EEG rhythms, exploring brain Small World characteristics, could predict—when combined with a genetic risk evaluation gleaned from the Apo-E genotype—the risk of conversion from MCI to AD as a first-level screening method with appropriate specificity/sensitivity. This type of combined approach (i.e. graph theory for EEG signals and

ApoE genotyping) have been previously utilized with *diagnostic* purposes in order to distinguish between healthy elderly and AD subjects<sup>31,32</sup>; however, to the best of our knowledge, such an approach has never been previously reported for *prognostic* purposes, namely to discriminate *prodromal-to-AD* from *non-prodromal* in a sample of MCI subjects.

Healthy brain organization reflects an optimal balance of functional integration and segregation; such a scenario is termed *small-world*. *Small World* characteristics reflect complex inhibitory and excitatory brain circuits consisting of functionally specialized regions that continuously and mutually cooperate to acquire, share and integrate information in a constant state of dynamic fluctuations that is also governed by a number of variables—including attention, emotion, motivation and arousal—influencing network performance. Connections between neuronal assemblies reflect segregation and integration processes, as revealed by local clustering (segregation) and path length (integration).

Here, a statistically significant difference in the SW organization of the Converted (particularly among rapid—i.e. within 1-2 years—converters) was found, and the Small World distributions in the EEG frequency bands of interest corresponded to a Stable aMCI; however, it was also shown that the Converted aMCI subjects do have SW characteristics very similar to those of Alzheimer’s patients 1 to 2 years before conversion (Time 0 of the study).

Many studies have looked at topological changes in the brain networks with different modalities and have examined the structural and diffusion tensor imaging MRI, EEG/MEG and fMRI recently reviewed by Xie & He<sup>52</sup>. Therefore, AD is more often considered a *disconnection syndrome*<sup>49</sup>, and brain topology can be represented by a progressive derangement of the brain organization in hub regions and long-range connections causing Small World architecture alteration. In fact, due to decreasing local and global connectivity parameters, the large-scale functional brain network organization in AD deviates from the optimal small-world architecture towards a more “ordered” type (as reflected by lower Small World values), leading to a less

efficient information exchange across brain areas that is in line with the disconnection hypothesis of Alzheimer's disease<sup>49</sup>.

Here, an abnormal increase in graph theory parameters in the Converted, with respect to the Stable MCI, has been observed for the low alpha rhythm, along with a decrease in the delta and gamma rhythms. Such an effect should be interpreted in light of the physiological role which the alpha rhythm plays. Alpha frequencies constitute the leading characteristic of normal EEG activity at waking rest, usually defined as the "idling rhythms" of the adult brain<sup>53</sup>. Several studies support the hypothesis that alpha is a deterministic chaotic signal with several functional correlates ranging from memory formation to sensory-motor processing<sup>54</sup>. In healthy individuals, alpha rhythm works as an oscillatory component of brain activity and can therefore be interpreted as a basic form of information transmission in the brain<sup>55</sup>. Moreover, event-related activity studies have shown a positive correlation between alpha frequency and the speed of information processing, as well as a good cognitive performance<sup>55</sup>.

For the delta band, it is argued that, in a waking state, such EEG rhythms are poorly represented, thus reflecting a condition of likely alpha-delta "reciprocal inhibition"<sup>11</sup>. Furthermore, it is well known that the anatomical or functional disconnection of lesioned cortical areas generates spontaneous slow oscillations in the delta range in virtually all recorded neurons. The SW decrease in the delta band represents a type of structured behavior that could be interpreted as an increase in delta activity and a functional inhibition. The opposite holds true for the alpha band.

A Small World decrease in the gamma band in the converted MCI is in line with previous evidence<sup>26</sup> showing a decrease of the Small World gamma band in Alzheimer's patients with respect to MCI and control subjects. The gamma band (>30 Hz) includes high-frequency EEG oscillations that mediate information transfer between cortical and hippocampal structures for memory processes<sup>56</sup>, particularly through feed-forward mechanisms<sup>57</sup> and coherent phase-coupling between oscillations from different structures<sup>58</sup>. Both animal and human studies

provide evidence that gamma oscillations play a fundamental role in memory tasks. Gamma neural activity is involved in numerous cognitive functions—including visual object processing, attention and memory<sup>59</sup>—and is also strongly associated with behavioral performance (accuracy and reaction time) in several memory tasks, including tasks probing episodic memory, encoding and retrieval<sup>60</sup>. Further, microelectrode intraneural recordings have demonstrated that gamma oscillations are pivotal in spike phase synchronization, which is at the base of EEG connectivity mechanisms<sup>61</sup>.

The ROC curve for EEG SW characteristics showed a >60% sensitivity (AUC 0.64, indicating moderate classification accuracy) for classifying the MCI state as a prodromal indicator of AD when all subjects were used. The present findings are in line with those of previous studies<sup>26,39,62</sup> in which Small World characteristics were found to have decreased in patients with AD with respect to MCI in low frequency EEG rhythms. In other words, the MCI connectivity pattern was less random than that of the AD group. Moreover, significant differences between healthy elderly MCI subjects and AD patients have been demonstrated by showing that physiological brain aging presents greater specialization (though lower values) of Small World EEG rhythm characteristics that are higher than normal in slow frequencies and lower in alpha bands<sup>28</sup>. Finally, the control analysis, with respect to AD patients, showed that Converted aMCI presented a graph theory pattern which was practically identical to that of AD. These findings suggest that EEG connectivity analysis, combined with neuropsychological evaluation in MCI, could be of great help in early identification of this condition as a first-line screening method and a means to intercept those subjects with a high risk for rapid progression to AD.

ROC curves showed that, when both phenotype and genotype characteristics (obtained at a low cost with widely available Apo-E technology) were combined, the accuracy remarkably increased to 91.78% (AUC 0.97, indicating an optimal classification accuracy) for classifying the MCI state as prodromal of AD. This result is in line with the fact that the  $\epsilon 4$  allele of the APO-E

gene is a major genetic risk factor for pathogenesis of late-onset Alzheimer's disease<sup>33,34</sup>; it also suggests that SW characteristics and Apo-E contribute to predict outcome in a synergistic way with little overlap. We also verified that the EEG Small World measures played a particularly relevant role in APO-E e4 non-carriers. Of note, a more homogenous population showed decreased accuracy, but it should be also noted that the more homogenous population consisted in a lower number of subjects.

Altogether, our findings clearly demonstrate that ApoE genotype and EEG connectivity reflect different types of “aggressors” responsible for neurodegenerative mechanisms and that they nicely integrate each other when considered in combination.

Is the "graph theoretical" model superior to other types of EEG analysis in an AD diagnostic context? In order to answer this question, we compared the same type of classifier to other methods of EEG analysis currently used for AD studies; we then applied the results to the same EEG epochs utilized for graph valuation, namely spectral coherence and power spectrum, still in combination with Apo-E genotyping. The analysis showed 51.79% sensitivity, 100% specificity and 68.86% accuracy. These results are promising but less significant than those from our Small World analysis.

The intrinsic characteristics of EEG rhythms contain relevant information on neurodegenerative processes underlying AD. These processes begin long before clinical symptoms manifest, by deranging the synaptic transmissions and the efficacy of brain dynamic connections<sup>49</sup>. A plastic reorganization of the surviving neuronal circuitries—the neural “reserve”—affects daily living abilities. This is due to prolonged neurodegeneration toward a network maintenance of functional connections<sup>11,49,63</sup>. In aMCI-C subjects, the Small World characteristics provided reliable predictions of aMCI to AD progression within a relatively short timeframe. Moreover, rapid progression from aMCI to AD heralds an aggressive type of dementia with a rapid degradation of daily life skills.

In conclusion, EEG connectivity analysis, combined with a neuropsychological MCI pattern and Apo-E genotyping, could represent a combination of biomarkers that are of great help in the early identification of MCI prodromal to AD. This combination represents a multimodal, low-cost and non-invasive approach, one that utilizes widely available techniques which, when combined, reach high sensitivity/specificity and good classification accuracy on an individual basis (higher than 0.97 of AUC). It could therefore be used to effectively determine the risk of the progression to AD in MCI patients and should be considered a first line of screening.

**Acknowledgements:** This work was partially supported by the Italian Ministry of Health for Institutional Research (Ricerca corrente) and for the project “NEUROMASTER: NEURONavigated MAgnetic STimulation in patients with mild-moderate Alzheimer’s disease, combined with Effective cognitive Rehabilitation” (GR-2013-02358430).

**Author contributions:** PMR, FV and FM: study concept and design; GL, VG, VFT, PP, FV, FM, FI and CM: data acquisition and analysis including statistical evaluation; FV, FM and PMR: drafting the manuscript and figures.

None of the authors have potential conflicts of interest to be disclosed

## Figures & Table Legends

**Table 1:** Clinical data of the two groups of aMCI: MMSE (mini mental state examination); RAVLT (Rey's Auditory Verbal Learning Test); MFTC (Multiple Features Target Cancellation); and StroopSf (Stroop test short form).

**Table 2:** Clinical data of the two homogeneous subgroups of aMCI (in the right, subjects having Apo-E): MMSE (mini mental state examination); RAVLT (Rey's Auditory Verbal Learning Test); MFTC (Multiple Features Target Cancellation); and StroopSf (Stroop test short form).

**Figure 1:** *Small World* characteristics across EEG frequency bands in Stable and Converted aMCI subjects with respect to AD patients.

**Figure 2:** Functional coupling in Stable and Converted subjects. An arbitrary threshold was used to illustrate these patterns. It is evident that Converted aMCI presented more coupling in delta and beta and gamma, and less coupling in alpha than Stable MCI.

**Figure 3:** Average receiver operating characteristic (ROC) curves and their confidence intervals, illustrating the classification of the Stable and Converted aMCI individuals based on the Apo-E (red line, 97 patients), *Small World* (green line, 145 patients) and Apo-E and EEG (blue line, 97 patients) values. The area under the ROC (AUC) curves was, respectively, 0.52, 0.64 and 0.97, indicating an optimal classification accuracy.

**Figure 4:** Square image representation Lagged Linear Coherence of each band in both pre and post. In the axes there are reported the single nodes of the network: BA 1F, 2P, 3F, 4F, 5P, 6F, 7P, 8F, 9F, 10F, 11F, 13F, 17O, 18O, 19O, 20T, 21T, 22T, 23P, 24F, 25F, 27T, 28T, 29T, 30T, 31P, 32F, 33F, 34T, 35T, 36T, 37T, 38T, 39P, 40P, 41T, 42T, 43P, 44F, 45F, 46F, 47F first in the left and then in the right hemisphere, where F, T, O and P represent Frontal, Temporal, Occipital and Parietal, respectively.

## References

1. Petersen,R.C., Smith,G.E., Ivnik,R.J., Tangalos,E.G., Schaid,D.J., Thibodeau,S.N., Kokmen,E., Waring,S.C., and Kurland,L.T. *Apolipoprotein E status as a predictor of the development of Alzheimer's disease in memory-impaired individuals*, JAMA **273**(16) 1274-1278 (1995).
2. Petersen,R.C., Doody,R., Kurz,A., Mohs,R.C., Morris,J.C., Rabins,P.V., Ritchie,K., Rossor,M., Thal,L., and Winblad,B. *Current concepts in mild cognitive impairment*, Arch. Neurol **58**(12) 1985-1992 (2001).
3. Scheltens,P., Fox,N., Barkhof,F., and De,C.C. *Structural magnetic resonance imaging in the practical assessment of dementia: beyond exclusion*, Lancet Neurol **1**(1) 13-21 (2002).
4. Petersen,R.C. *Mild cognitive impairment as a diagnostic entity*, J Intern. Med. **256**(3) 183-194 (2004).
5. Petersen,R.C. et al. *Practice guideline update summary: Mild cognitive impairment: Report of the Guideline Development, Dissemination, and Implementation Subcommittee of the American Academy of Neurology*, Neurology **90**(3) 126-135 (2018).
6. Nathan,P.J. et al. *Association between CSF biomarkers, hippocampal volume and cognitive function in patients with amnesic mild cognitive impairment (MCI)*, Neurobiol. Aging **53** 1-10 (2017).
7. Roberts,R. and Knopman,D.S. *Classification and epidemiology of MCI*, Clin. Geriatr. Med. **29**(4) 753-772 (2013).
8. Getsios,D., Blume,S., Ishak,K.J., Maclaine,G., and Hernandez,L. *An economic evaluation of early assessment for Alzheimer's disease in the United Kingdom*, Alzheimers. Dement. **8**(1) 22-30 (2012).
9. Wimo,A., Jonsson,L., Bond,J., Prince,M., and Winblad,B. *The worldwide economic impact of dementia 2010*, Alzheimers. Dement. **9**(1) 1-11 (2013).
10. Vecchio,F., Babiloni,C., Lizio,R., Fallani,F., V, Blinowska,K., Verrienti,G., Frisoni,G., and Rossini,P.M. *Resting state cortical EEG rhythms in Alzheimer's disease: toward EEG markers for clinical applications: a review*, Suppl Clin. Neurophysiol **62** 223-236 (2013).
11. Rossini,P.M. et al. *Conversion from mild cognitive impairment to Alzheimer's disease is predicted by sources and coherence of brain electroencephalography rhythms*, Neuroscience **143**(3) 793-803 (2006).
12. Huang,C., Wahlund,L., Dierks,T., Julin,P., Winblad,B., and Jelic,V. *Discrimination of Alzheimer's disease and mild cognitive impairment by equivalent EEG sources: a cross-sectional and longitudinal study*, Clin. Neurophysiol **111**(11) 1961-1967 (2000).
13. Koenig,T., Prichep,L., Dierks,T., Hubl,D., Wahlund,L.O., John,E.R., and Jelic,V. *Decreased EEG synchronization in Alzheimer's disease and mild cognitive impairment*, Neurobiol. Aging **26**(2) 165-171 (2005).
14. Jelic,V., Johansson,S.E., Almkvist,O., Shigeta,M., Julin,P., Nordberg,A., Winblad,B., and Wahlund,L.O. *Quantitative electroencephalography in mild cognitive*

*impairment: longitudinal changes and possible prediction of Alzheimer's disease*, Neurobiol. Aging **21**(4) 533-540 (2000).

15. Adler,G., Brassens,S., and Jajcevic,A. *EEG coherence in Alzheimer's dementia*, J Neural Transm. (Vienna. ) **110**(9) 1051-1058 (2003).

16. Prichep,L.S., John,E.R., Ferris,S.H., Rausch,L., Fang,Z., Cancro,R., Torossian,C., and Reisberg,B. *Prediction of longitudinal cognitive decline in normal elderly with subjective complaints using electrophysiological imaging*, Neurobiol. Aging **27**(3) 471-481 (2006).

17. de Haan,W., Mott,K., van Straaten,E.C., Scheltens,P., and Stam,C.J. *Activity dependent degeneration explains hub vulnerability in Alzheimer's disease*, PLoS. Comput. Biol **8**(8) e1002582 (2012).

18. Dauwels,J., Vialatte,F., and Cichocki,A. *Diagnosis of Alzheimer's disease from EEG signals: where are we standing?*, Curr. Alzheimer Res. **7**(6) 487-505 (2010).

19. Babiloni,C., Vecchio,F., Lizio,R., Ferri,R., Rodriguez,G., Marzano,N., Frisoni,G.B., and Rossini,P.M. *Resting state cortical rhythms in mild cognitive impairment and Alzheimer's disease: electroencephalographic evidence*, J Alzheimers. Dis. **26 Suppl 3** 201-214 (2011).

20. Vecchio,F., Miraglia,F., Quaranta,D., Granata,G., Romanello,R., Marra,C., Bramanti,P., and Rossini,P.M. *Cortical connectivity and memory performance in cognitive decline: a study via graph theory from EEG data*, Submitted to Neuroscience (2015).

21. Vecchio,F., Miraglia,F., Piludu,F., Granata,G., Romanello,R., Caulo,M., Onofrj,V., Bramanti,P., Colosimo,C., and Rossini,P.M. *"Small World" architecture in brain connectivity and hippocampal volume in Alzheimer's disease: a study via graph theory from EEG data*, Brain Imaging Behav. (2016).

22. Dauwels,J., Vialatte,F., Musha,T., and Cichocki,A. *A comparative study of synchrony measures for the early diagnosis of Alzheimer's disease based on EEG*, Neuroimage. **49**(1) 668-693 (2010).

23. Friston,K.J. *Functional and effective connectivity in neuroimaging: A synthesis*, Human Brain Mapping **2** 56-78 (1994).

24. Watts,D.J. and Strogatz,S.H. *Collective dynamics of 'small-world' networks*, Nature **393**(6684) 440-442 (1998).

25. Bassett,D.S. and Bullmore,E. *Small-world brain networks*, Neuroscientist. **12**(6) 512-523 (2006).

26. Vecchio,F., Miraglia,F., Marra,C., Quaranta,D., Vita,M.G., Bramanti,P., and Rossini,P.M. *Human brain networks in cognitive decline: a graph theoretical analysis of cortical connectivity from EEG data*, J Alzheimers. Dis. **41**(1) 113-127 (2014).

27. Vecchio,F., Miraglia,F., Bramanti,P., and Rossini,P.M. *Human brain networks in physiological aging: a graph theoretical analysis of cortical connectivity from EEG data*, J Alzheimers. Dis. **41**(4) 1239-1249 (2014).

28. Vecchio,F., Miraglia,F., Curcio,G., Altavilla,R., Scrascia,F., Giambattistelli,F., Quattrocchi,C.C., Bramanti,P., Vernieri,F., and Rossini,P.M. *Cortical Brain Connectivity*

*Evaluated by Graph Theory in Dementia: A Correlation Study Between Functional and Structural Data*, J Alzheimers. Dis. (2015).

29. Stam,C.J., Jones,B.F., Nolte,G., Breakspear,M., and Scheltens,P. *Small-world networks and functional connectivity in Alzheimer's disease*, Cereb. Cortex **17**(1) 92-99 (2007).

30. de Haan,W., Pijnenburg,Y.A., Strijers,R.L., van der Made,Y., van der Flier,W.M., Scheltens,P., and Stam,C.J. *Functional neural network analysis in frontotemporal dementia and Alzheimer's disease using EEG and graph theory*, BMC. Neurosci. **10** 101 (2009).

31. Kramer,G., van der Flier,W.M., de,L.C., Blankenstein,M.A., Scheltens,P., and Stam,C.J. *EEG functional connectivity and ApoE genotype in Alzheimer's disease and controls*, Clin. Neurophysiol **119**(12) 2727-2732 (2008).

32. Canuet,L., Tellado,I., Couceiro,V., Fraile,C., Fernandez-Novoa,L., Ishii,R., Takeda,M., and Cacabelos,R. *Resting-state network disruption and APOE genotype in Alzheimer's disease: a lagged functional connectivity study*, PLoS. One. **7**(9) e46289 (2012).

33. Huang,Y. and Mucke,L. *Alzheimer mechanisms and therapeutic strategies*, Cell **148**(6) 1204-1222 (2012).

34. Giri,M., Zhang,M., and Lu,Y. *Genes associated with Alzheimer's disease: an overview and current status*, Clin. Interv. Aging **11** 665-681 (2016).

35. Winblad,B. et al. *Mild cognitive impairment--beyond controversies, towards a consensus: report of the International Working Group on Mild Cognitive Impairment*, J Intern. Med. **256**(3) 240-246 (2004).

36. McKhann,G.M. et al. *The diagnosis of dementia due to Alzheimer's disease: recommendations from the National Institute on Aging-Alzheimer's Association workgroups on diagnostic guidelines for Alzheimer's disease*, Alzheimers. Dement. **7**(3) 263-269 (2011).

37. Petersen,R.C., Smith,G.E., Waring,S.C., Ivnik,R.J., Kokmen,E., and Tangelos,E.G. *Aging, memory, and mild cognitive impairment*, Int. Psychogeriatr. **9 Suppl 1** 65-69 (1997).

38. Portet,F., Ousset,P.J., Visser,P.J., Frisoni,G.B., Nobili,F., Scheltens,P., Vellas,B., and Touchon,J. *MCI Working Group of the European Consortium on Alzheimer's Disease Mild cognitive impairment (MCI) in medical practice: a critical review of the concept and new diagnostic procedure. Report of the MCI Working Group of the European Consortium on Alzheimer's Disease*. J Neurol Neurosurg Psychiatry **77** 714-718 (2006).

39. Miraglia,F., Vecchio,F., Bramanti,P., and Rossini,P.M. *EEG characteristics in "eyes-open" versus "eyes-closed" conditions: Small-world network architecture in healthy aging and age-related brain degeneration*, Clin. Neurophysiol **127**(2) 1261-1268 (2016).

40. Miraglia,F., Vecchio,F., and Rossini,P.M. *Searching for signs of aging and dementia in EEG through network analysis*, Behav. Brain Res. **317** 292-300 (2017).

41. Pascual-Marqui,R.D. *Standardized low-resolution brain electromagnetic tomography (sLORETA): technical details*, Methods Find. Exp. Clin. Pharmacol. **24 Suppl D** 5-12 (2002).

42. Pascual-Marqui,R.D. *Instantaneous and lagged measurements of linear and nonlinear dependence between groups of multivariate time series: frequency decomposition.*, arXiv preprint arXiv:0711. 1455. (2007).
43. Rubinov,M. and Sporns,O. *Complex network measures of brain connectivity: uses and interpretations*, Neuroimage. **52**(3) 1059-1069 (2010).
44. Hixson,J.E. and Vernier,D.T. *Restriction isotyping of human apolipoprotein E by gene amplification and cleavage with HhaI*, J Lipid Res. **31**(3) 545-548 (1990).
45. Lehmann,D., Faber,P.L., Tei,S., Pascual-Marqui,R.D., Milz,P., and Kochi,K. *Reduced functional connectivity between cortical sources in five meditation traditions detected with lagged coherence using EEG tomography*, Neuroimage. **60**(2) 1574-1586 (2012).
46. Barnett,J.H., Lewis,L., Blackwell,A.D., and Taylor,M. *Early intervention in Alzheimer's disease: a health economic study of the effects of diagnostic timing*, BMC. Neurol **14** 101 (2014).
47. Wimo,A., Guerchet,M., Ali,G.C., Wu,Y.T., Prina,A.M., Winblad,B., Jonsson,L., Liu,Z., and Prince,M. *The worldwide costs of dementia 2015 and comparisons with 2010*, Alzheimers. Dement. **13**(1) 1-7 (2017).
48. Teipel,S.J., Kurth,J., Krause,B., and Grothe,M.J. *The relative importance of imaging markers for the prediction of Alzheimer's disease dementia in mild cognitive impairment - Beyond classical regression*, Neuroimage. Clin. **8** 583-593 (2015).
49. D'Amelio,M. and Rossini,P.M. *Brain excitability and connectivity of neuronal assemblies in Alzheimer's disease: from animal models to human findings*, Prog. Neurobiol. **99**(1) 42-60 (2012).
50. Petersen,R.C., Thomas,R.G., Aisen,P.S., Mohs,R.C., Carrillo,M.C., and Albert,M.S. *Randomized controlled trials in mild cognitive impairment: Sources of variability*, Neurology **88**(18) 1751-1758 (2017).
51. Sachdev,P.S. et al. *The Prevalence of Mild Cognitive Impairment in Diverse Geographical and Ethnocultural Regions: The COSMIC Collaboration*, PLoS. One. **10**(11) e0142388 (2015).
52. Xie,T. and He,Y. *Mapping the Alzheimer's brain with connectomics*, Front Psychiatry **2** 77 (2011).
53. Niedermeyer,E. and da Silva,F.L. *Electroencephalography: Basic Principles, Clinical Applications, and Related Fields*Lippincott Williams & Wilkins). (2005).
54. Schurmann,M. and Basar,E. *Functional aspects of alpha oscillations in the EEG*, Int. J. Psychophysiol. **39**(2-3) 151-158 (2001).
55. Klimesch,W. *EEG alpha and theta oscillations reflect cognitive and memory performance: a review and analysis*, Brain Res. Brain Res. Rev. **29**(2-3) 169-195 (1999).
56. Vinck,M., Womelsdorf,T., Buffalo,E.A., Desimone,R., and Fries,P. *Attentional modulation of cell-class-specific gamma-band synchronization in awake monkey area v4*, Neuron **80**(4) 1077-1089 (2013).

57. Abeles, M. *Corticonics: neural circuits of the cerebral cortex.*, New York: Cambridge UP (1991).
58. Fries, P. *A mechanism for cognitive dynamics: neuronal communication through neuronal coherence*, Trends Cogn Sci. **9**(10) 474-480 (2005).
59. Tallon-Baudry, C., Bertrand, O., Peronnet, F., and Pernier, J. *Induced gamma-band activity during the delay of a visual short-term memory task in humans*, J Neurosci. **18**(11) 4244-4254 (1998).
60. Kaiser, J., Heidegger, T., and Lutzenberger, W. *Behavioral relevance of gamma-band activity for short-term memory-based auditory decision-making*, Eur. J Neurosci. **27**(12) 3322-3328 (2008).
61. Nikolic, D., Fries, P., and Singer, W. *Gamma oscillations: precise temporal coordination without a metronome*, Trends Cogn Sci. **17**(2) 54-55 (2013).
62. de Haan, W., van der Flier, W.M., Koene, T., Smits, L.L., Scheltens, P., and Stam, C.J. *Disrupted modular brain dynamics reflect cognitive dysfunction in Alzheimer's disease*, Neuroimage. **59**(4) 3085-3093 (2012).
63. Ferreri, F., Pauri, F., Pasqualetti, P., Fini, R., Dal, F.G., and Rossini, P.M. *Motor cortex excitability in Alzheimer's disease: a transcranial magnetic stimulation study*, Ann. Neurol **53**(1) 102-108 (2003).

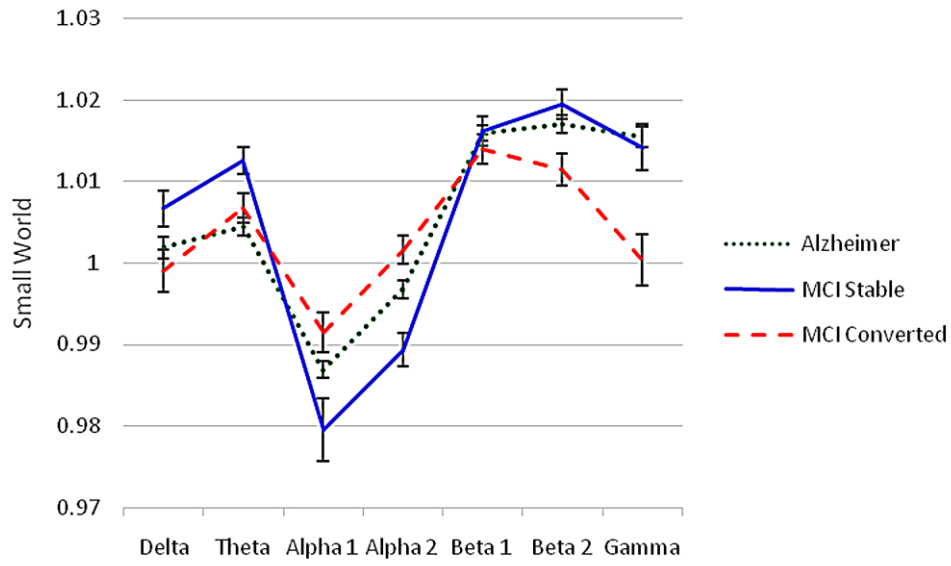


**Figure 1:** *Small World* characteristics across EEG frequency bands in Stable and Converted aMCI subjects with respect to AD patients.

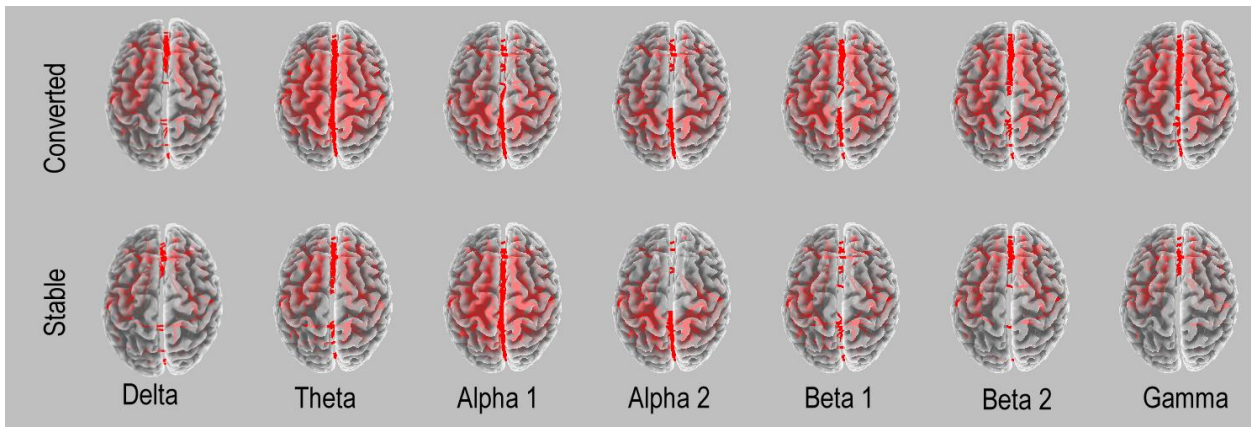


**Figure 2:** Functional coupling in Stable and Converted subjects. An arbitrary threshold was used to illustrate these patterns. It is evident that Converted aMCI presented more coupling in delta and beta and gamma, and less coupling in alpha than Stable MCI.

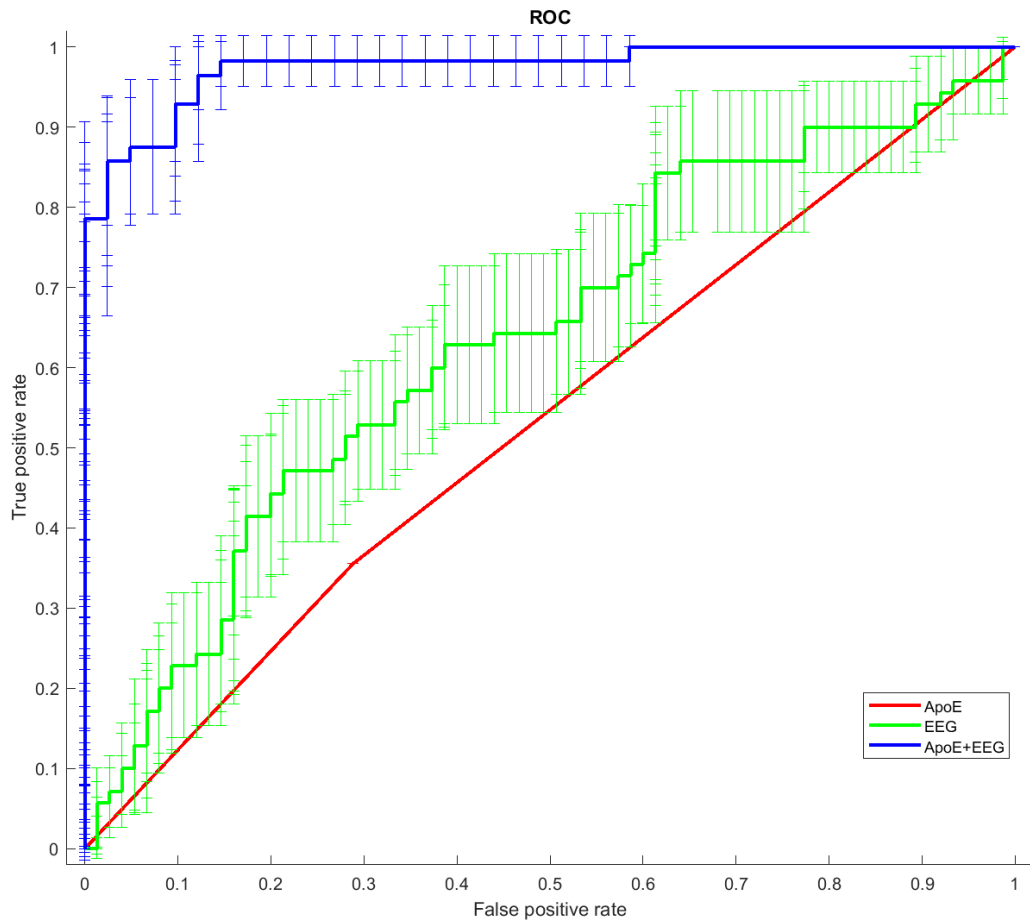


**Figure 3:** Average receiver operating characteristic (ROC) curves and their confidence intervals, illustrating the classification of the Stable and Converted aMCI individuals based on the Apo-E (red line, 97 patients), *Small World* (green line, 145 patients) and Apo-E and EEG (blue line, 97 patients) values. The area under the ROC (AUC) curves was, respectively, 0.52, 0.64 and 0.97, indicating an optimal classification accuracy.

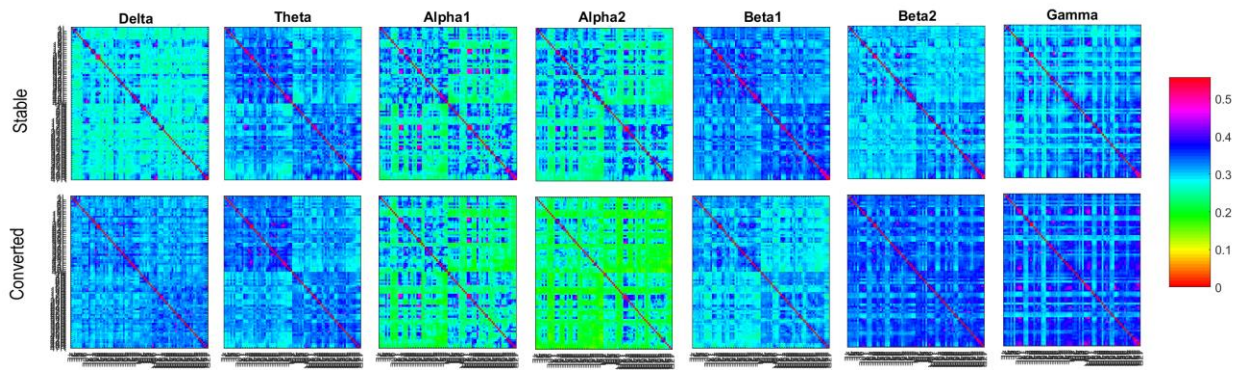


**Figure 4:** Square image representation Lagged Linear Coherence of each band in both pre and post. In the axes there are reported the single nodes of the network: BA 1F, 2P, 3F, 4F, 5P, 6F, 7P, 8F, 9F, 10F, 11F, 13F, 17O, 18O, 19O, 20T, 21T, 22T, 23P, 24F, 25F, 27T, 28T, 29T, 30T, 31P, 32F, 33F, 34T, 35T, 36T, 37T, 38T, 39P, 40P, 41T, 42T, 43P, 44F, 45F, 46F, 47F first in the left and then in the right hemisphere, where F, T, O and P represent Frontal, Temporal, Occipital and Parietal, respectively.

**Table 1**

	<b>Stable</b>			<b>Converted</b>	
	Mean	St Err		Mean	St Err
Educational level	10,15	0,71		10,02	0,70
RAVLT Immediate Recall	26,95	1,19		24,50	0,99
RAVLT Delayed Recall	3,87	0,49		2,32	0,34
RAVLT Recognition corr.	10,34	0,53		9,06	0,72
RAVLT Recognition False	4,97	0,97		4,31	1,00
RAVLT Recognition Accuracy	0,85	0,02		0,81	0,03
Constructional Praxis	9,26	0,36		8,59	0,41
Constructional Praxis Landmarks	66,26	0,75		64,85	1,03
MFTC Accuracy	0,96	0,01		0,90	0,02
MFTC False alarms	0,43	0,18		1,55	0,65
MFTC time	95,96	5,04		96,52	9,29
Raven' Matrices '47	24,53	0,99		25,13	2,84
Phonological Verbal Fluency	30,57	1,94		25,09	1,38
Categorical Verbal Fluency	10,96	0,83		10,52	0,65
StroopSf interference Time	33,71	3,93		55,52	9,19
StroopSf Interference Errors	1,89	0,58		5,19	1,56
Corsi Forward	4,69	0,26		3,71	0,39
Corsi Backward	3,50	0,29		3,60	0,24
Clock-Drawing	3,13	0,44		2,43	0,53
Prose Memory	3,63	1,08		1,43	0,57
Span Forward	5,23	0,30		5,22	0,32
Span Backward	4,00	0,41		3,17	0,40

Clinical data of the two groups of aMCI: MMSE (mini mental state examination); RAVLT (Rey's Auditory Verbal Learning Test); MFTC (Multiple Features Target Cancellation); and StroopSf (Stroop test short form).

**Table 2**

	42 Stable		43 Converted		27 Stable		30 Converted	
	Mean	St Err	Mean	St Err	Mean	St Err	Mean	St Err
MMSE	26.09	0.34	25.63	0.27	26.60	0.39	25.47	0.36
age	71.71	0.89	72.02	1.05	71.15	1.00	72.27	1.12
Educational level	9.36	0.75	10.07	0.79	9.56	0.91	9.83	0.93
RAVLT Immediate Recall	25.91	1.23	25.38	1.07	26.24	1.56	25.90	1.42
RAVLT Delayed Recall	2.97	0.43	2.61	0.44	3.05	0.55	2.92	0.56
RAVLT Recognition corr.	10.41	0.58	9.73	0.70	9.76	0.81	9.65	1.03
RAVLT Recognition False	5.36	1.02	5.35	1.24	5.25	0.93	6.24	1.76
RAVLT Recognition Accuracy	0.82	0.02	0.83	0.02	0.83	0.02	0.82	0.03
Constructional Praxis	9.16	0.28	9.00	0.38	8.87	0.35	8.08	0.35
Constructional Praxis Landmarks	66.00	0.60	64.55	1.10	65.93	0.82	62.54	1.48
MFTC Accuracy	0.97	0.01	0.91	0.02	0.97	0.01	0.90	0.03
MFTC False alarms	1.24	0.72	1.25	0.47	1.44	1.01	1.35	0.58
MFTC time	79.38	5.61	81.64	6.13	83.19	7.14	82.07	8.47
Raven' Matrices '47	24.88	1.02	22.44	1.06	25.10	1.35	21.98	1.33
Phonological Verbal Fluency	29.00	1.55	28.13	1.44	27.80	1.92	28.56	2.00
Categorical Verbal Fluency	13.30	0.71	10.87	0.74	12.94	0.90	11.69	0.94
Stroopsf interference Time	41.54	5.99	42.50	6.86	36.55	5.18	37.54	5.00
Stroopsf Interference Errors	2.18	0.54	2.55	0.56	3.10	0.56	3.13	0.76
Corsi Forward	4.70	0.19	4.25	0.17	5.50	0.47	4.67	0.13
Corsi Backward	3.50	0.13	3.33	0.11	3.50	0.16	3.33	0.13
Clock-Drawing	3.13	0.23	3.17	0.18	3.14	0.30	3.20	0.24
Span Forward	5.20	0.21	5.00	0.23	5.00	0.32	5.00	0.32
Span Backward	4.00	0.26	3.50	0.18	3.50	0.47	3.50	0.22

Clinical data of the two homogeneous subgroups of aMCI (in the right, subjects having Apo-E): MMSE (mini mental state examination); RAVLT (Rey's Auditory Verbal Learning Test); MFTC (Multiple Features Target Cancellation); and StroopSf (Stroop test short form).